Supplementary Information

Annexin-A5 assembled into two-dimensional arrays promotes cell membrane repair

Anthony Bouter, Céline Gounou, Rémi Bérat, Sisareuth Tan, Bernard Gallois, Thierry Granier, Béatrice Langlois d'Estaintot, Ernst Pöschl, Bent Brachvogel, Alain R. Brisson

Supplementary Figures

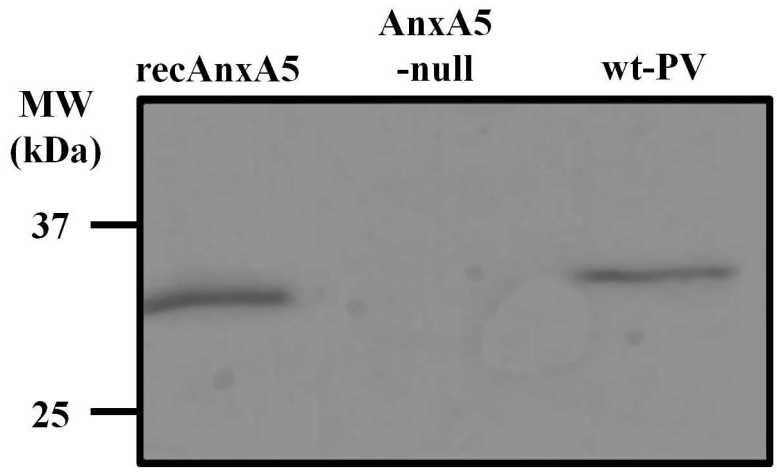

Supplementary Figure S1. AnxA5 content of wt-PV and AnxA5-null PV cells.

The cellular content of AnxA5 in AnxA5-null PV (middle) and wt-PV (right) cells was quantified by immunoblot analysis, by comparison with purified recombinant AnxA5 (recAnxA5) (left). (left), 50 ng recAnxA5; (middle) and (right), 20 µg protein extract from AnxA5-null PV and wt-PV cells, respectively. AnxA5 was detected with a rabbit anti-AnxA5 polyclonal antibody (Abcam). The AnxA5 contents of AnxA5-null PV and wt-PV cells were estimated at 0 and 1.8 µg/mg total protein, respectively.

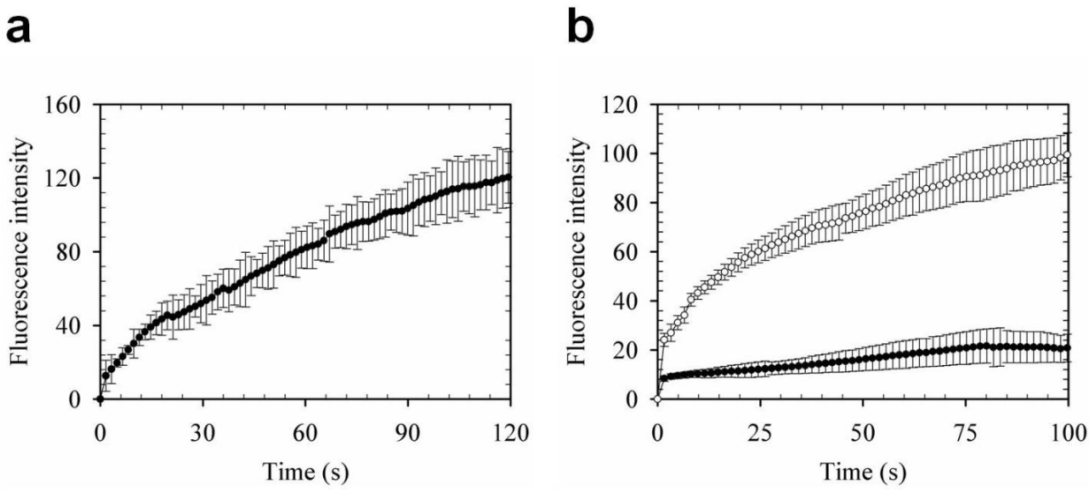

Supplementary Figure S2. Kinetics of FM1-43 fluorescence intensity increase.

(a) wt-PV cells after membrane damage at 160 mW IR-irradiation in the presence of 1 mM EGTA.

(b) wt-PV cells (filled circles) and AnxA5-null PV cells (empty circles) after membrane damage at 80 mW IR-irradiation in the presence of 2 mM Ca^{2+}.

Data represent the fluorescence intensity integrated over whole cell sections, averaged for 10 cells (+/- SD).

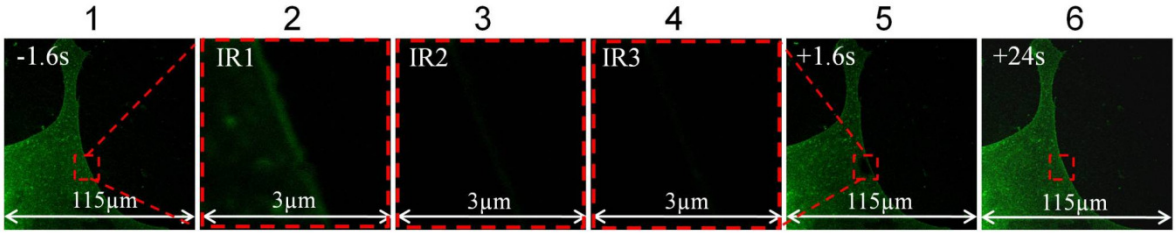

Supplementary Figure S3. Photobleaching of FM1-43 at the irradiated membrane site. Representative image series showing the response a wt-PV cell to 80 mW-irradiation. This cell (same cell as presented in Fig. 3c) belongs to the major population (~70%) of wt-PV cells that show no increase of fluorescence intensity after irradiation. Image (1) represents a full-size image (115 µm x 115 µm) which was recorded 1.6s prior irradiation. Images (2-4), marked IR1 to IR3, represent the 3µm x 3µm irradiated area, recorded during the three consecutive IR scans of 1.6s each. Images 5 and 6 represent full-size images (115 µm x 115 µm) which were recorded 1.6s and 24s after irradiation, respectively. A red dashed box in images (1), (5) and (6) surrounds an area slightly larger than the 3µm x 3µm irradiated area. Images (2-4) show a progressive fading of the fluorescence intensity, with a complete photobleaching of FM1-43 dyes in (4). The total photobleaching of FM1-43 dyes within the irradiation area at the end of the irradiation step indicates that the cell was correctly focused. All cells analyzed in this study presented this behavior.

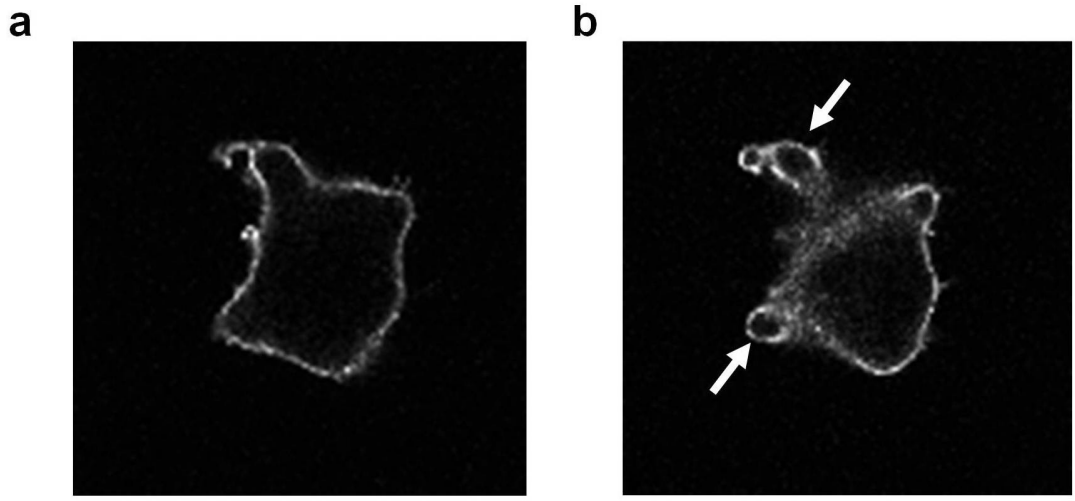

Supplementary Figure S4. Binding of Cy5-AnxA5 to apoptotic wt-PV cells.

Fluorescence images of an apoptotic wt-PV cell incubated with Cy5-AnxA5. Images were recorded at 3.7 µm (**a**) and 4.8 µm (**b**) above the supporting glass slide. Cell death was induced by incubation for 1h at ambient temperature in HBS-Ca, pH 7.4; HBS contains 2 mM NaN_3, which is responsible for apoptosis. The cells were then incubated for 5 min in HBS-Ca supplemented with 3µg/mL Cy5-AnxA5 and then washed with HBS-Ca before imaging. The entire cell surface is labeled with Cy5-AnxA5, in agreement with the fact that apoptotic cells present a homogenous distribution of cell surface-exposed PS molecules[61]. The presence of blebs (white arrows in section (**b**) is characteristic of apoptotic cells[62].

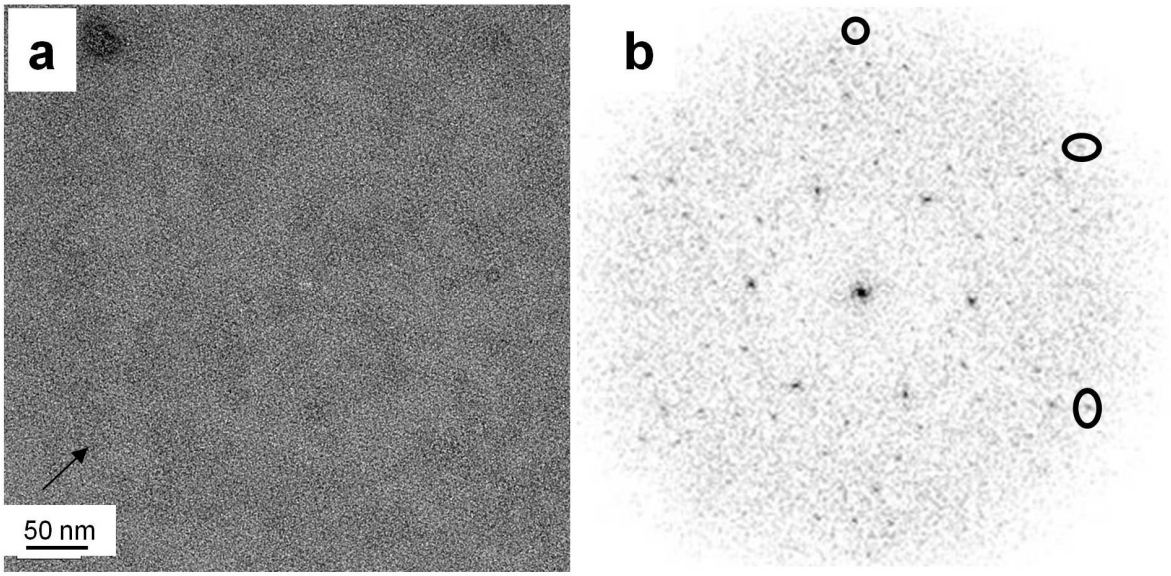

Supplementary Figure S5. TEM analysis of 2D assemblies of membrane-bound AnxA5.

(a) TEM image of a 2D crystal of native AnxA5 formed on a PS-containing lipid monolayer. The crystalline organization is better visible by viewing the image at glancing angle along the arrow.

(**b**) Typical Fourier transform of a p6 2D crystal of native AnxA5. The Fourier transform, calculated from an image area of about 200 nm x 200 nm, presents maxima localized on a hexagonal lattice. Strong maxima extend up to 1/3 nm^{-1} (circled). As AnxA5 2D crystals are based on AnxA5 trimers, the analysis of image Fourier transforms constitutes the most direct method for establishing the presence or absence of AnxA5 trimers. Essentially identical Fourier transforms were obtained with all single, double and triple mutants of AnxA5. Contrarily, Fourier transforms calculated from all the images obtained with quadruple and quintuple AnxA5 mutants were characterized by the total absence of diffraction maxima. This establishes that these mutants, including the mtT-AnxA5 quintuple mutant, do not form trimers and 2D arrays.

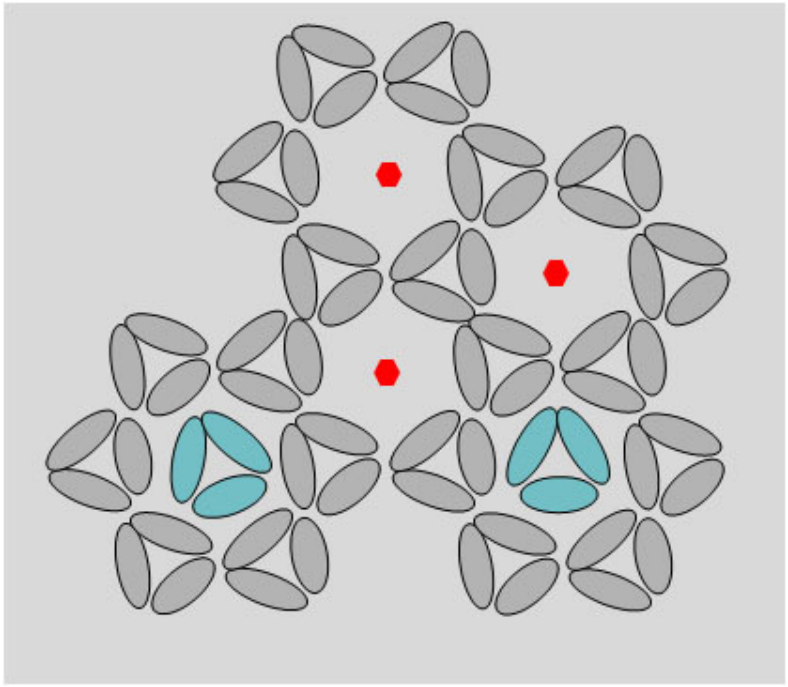

Supplementary Figure S6. Large open spaces within AnxA5 p6 2D crystals.

Model of a p6 2D crystal of AnxA5[29,35] showing the presence of large open spaces around the 6-fold symmetry centers (three 6-fold symmetry centers are indicated by red hexagons). These open spaces, of about 9-nm in diameter, are large enough for hosting additional AnxA5 trimers, as observed by AFM on model membranes[29], or possibly other proteins. Two AnxA5 trimers (colored in blue) have been incorporated to the 2D crystal, with arbitrary orientations.

Supplementary Table

Supplementary Table S1. X-ray diffraction data collection and refinement statistics.

Data collection	
Space group	$P2_1$
Cell dimensions	
a,b,c (Å)	51.108, 67.184, 112.313
α, β, γ (°)	90.0, 94.79, 90.0
Resolution (Å)	19.55 – 2.76 (2.91 – 2.76)[a]
R_{sym} (%)[b]	0.134 (0.374)
I/σI	5.3 (2.0)
Completeness (%)	97.1 (88.8)
Redundancy	3.2 (2.9)
Refinement	
Resolution (Å)	18.25 - 2.76 (2.83 – 2.76)
No. reflections	18179 (1173)
R_{work}(%)	0.197 (0.272)
No. atoms	
Protein	5007
Ligand/ion	22
Water	139
B-factors (Å^2)	
Protein	34.5
Ligand/ion	30.7
Water	24.9
R.m.s deviations	0.010
Bond lengths (Å)	0.010
Bond angles (°)	1.48
R_{work} /R_{free}	0.197 / 0.266

Supplementary Methods

Materials

FM1-43, DMEM, Dulbecco's phosphate buffer saline (DPBS) and cell culture reagents were from Invitrogen. HEPES, tris(hydroxymethyl)aminomethane (Tris), Tris(2-carboxy-ethyl)phosphine hydrochloride (TCEP) and fluorescein-di-ß-D-galactopyranoside were from Sigma-Aldrich. Cy5-N-ethylmaleimide was from GE-Healthcare. 1,2-dioleoyl-*sn*-glycero-3-phosphocholine (DOPC) and 1,2-dioleoyl-*sn*-glycero-3-[phospho-L-serine] (DOPS) were from Avanti Polar Lipids (Alabaster, AL). All other chemicals were of ultrapure grade. Water was purified with a RiOs system (Millipore, France).

3D crystallization of mtT-AnxA5 and structure analysis

MtT-AnxA5 was crystallized using the vapor diffusion method with hanging drops in Linbro plates. Crystals were grown at ambient temperature over 1.0 mL reservoir solution containing 7% PEG-8000, 75 mM calcium acetate, 100 mM sodium cacodylate, pH 6.4, 3 mM NaN_3 in drops composed of equal volumes (1 µL) of protein solution (5 mg/mL in 25 mM NaCl, 10 mM Tris, pH 8.0, 3 mM NaN_3) and reservoir solution. Crystals grew to their final size within 5 weeks.

X-ray diffraction experiments were performed on crystals cryo-protected in 40% glycerol, using a CuK_α radiation source generated from an Enraf-Nonius FR571 rotating anode. Data were collected at 100 K on a 300 mm MAR Research image plate scanner. All programs used for data processing, structure determination and refinement were from the CCP4 suite[63], with the exception of molecular graphics Turbo-Frodo[64]. Collected data were

processed with the program MOSFLM and scaled with the program SCALA. Diffraction data were indexed and processed in the $P2_1$ space group with lattice parameters a = 51.108 Å, b = 67.184 Å, c = 112.313 Å, $\beta = 94.79°$.

The structure of mtT-AnxA5 was determined by molecular replacement using recombinant rat AnxA5 as starting model[65] (atomic coordinates from PDB code 1a8a) with the program MOLREP. The asymmetric unit contains two protein molecules related to one another by a non crystallographic 2_ε screw axis parallel to the **a** axis with a non fractional pitch of $\varepsilon = 4.7$ Å (**Fig. 5c**).

Structure building and refinement were carried out with Turbo-Frodo and REFMAC, including TLS (Translation, Libration, Screw rotation) refinement. The refinement statistics are listed in Supplementary Table S1. The final SigmaA weighted (2mFo – DFc) map contoured at 1 σ displays continuous electron density along the main chain atoms of residues 2 to 319 for both molecules. A Ramachandran plot shows that 98% and 99.7% of the residues belong to favored regions and allowed regions, respectively.

Atomic coordinates and structure factor amplitudes of mtT-AnxA5 have been deposited to the RCSB Protein Data Bank with entry code 2h0k.

Supplementary References

61. Martin, S.J. et al. Early redistribution of plasma membrane phosphatidylserine is a general feature of apoptosis regardless of the initiating stimulus: inhibition by overexpression of Bcl-2 and Abl. *J. Exp. Med* **182**, 1545-1556 (1995).
62. Verhoven, B., Schlegel, R.A. & Williamson, P. Mechanisms of phosphatidylserine exposure, a phagocyte recognition signal, on apoptotic T lymphocytes. *J. Exp. Med* **182**, 1597-1601 (1995).
63. Collaborative Computational Project, Number 4 The CCP4 suite: programs for protein crystallography. *Acta Crystallogr D Biol Crystallogr* **50**, 760-763 (1994).
64. Roussel, A., Fontecilla-Camps, J. & Cambillau, C. Turbo-Frodo: a new program for protein crystallography and modeling. *Acta crystallographica. Section D, Biological crystallography* **46**, C66-C67 (1990).
65. Swairjo, M.A., Concha, N.O., Kaetzel, M.A., Dedman, J.R. & Seaton, B.A. Ca(2+)-bridging mechanism and phospholipid head group recognition in the membrane-binding protein annexin V. *Nat. Struct. Biol* **2**, 968-974 (1995).